Sliding Friction and Wear of Ceramics With and Without Soft Metallic Films

Ali Erdemir, Fred A. Nichols, George R. Fenske, and Jang-Hsing Hsieh

Introduction

In unlubricated sliding contact, essentially all the mechanical work done to overcome friction is converted into heat produced in the vicinity of real contacts. The amount of frictional heat flux q is proportional to the friction coefficient μ, the normal force F, and the sliding velocity v, but is inversely proportional to the nominal contact area A_n (e.g., $q = (\mu \times F \times v)/A_n$).[1-3] The real areas of contact, being much smaller than the nominal contact area, give rise to much higher local heat fluxes in the vicinity of asperity contacts. Because the frictional heat flux enters the contacting bodies through these regions (or locations known as "hot spots"), their local temperatures (referred to as "flash temperature") can be much higher than the overall or "bulk" surface temperature, as discussed in References 1–3.

Previous studies have demonstrated that frictional heat can profoundly affect the friction and wear behavior of both metallic and ceramic materials. In most steels[4] and nonoxide ceramics,[5,6] frictional heat was found to foster oxidation. The occurrence of phase transformations on or near the sliding surfaces was also cited in the literature for certain steels[7] and ZrO_2-based ceramics.[8,9]

Except for SiC, BeO, and AlN, most ceramics have significantly lower thermal conductivity than do metals. When in sliding contact, ceramics cannot dissipate frictional heat generated at sliding interfaces as effectively as most metallic alloys. Large temperature gradients can often develop between areas of real contact and surrounding regions, thus creating high thermal stresses. When these thermal stresses are combined with normal and tangential stresses (due to applied load and frictional traction), plastic yielding may occur and can produce wear;[2,3] alternatively, these brittle ceramics may fracture and hence may suffer severe wear losses. Plastic flow due to thermal softening and local melting may also occur and govern the wear behavior of ceramics.[11]

In recent papers, we have demonstrated that silver can be an effective solid lubricant for insulating ceramics.[11-13] Silver has a very high thermal conductivity (e.g., at 298 K, $k_{silver} = 429$ W/m · K). Moreover, it is relatively soft and chemically inert, thus can shear easily to reduce friction, and can resist oxidation when used in open air and elevated temperatures. The purpose of this study is to further explore the effectiveness of silver in controlling the wear of magnesia-partially stabilized zirconia (MgO-PSZ), especially at high sliding velocities where frictional heat becomes pronounced. Magnitudes of expected flash temperatures are displayed in temperature maps generated by the *T-MAPS* software of Ashby et al.[1] The chemical and structural changes at the sliding interfaces are examined microscopically and correlated with the flash-temperature estimates.

Experimental Details

Test Materials

The pin and disk specimens were prepared from Nilcra grade MS MgO-PSZ comprising ≈4.3% monoclinic, 24.4% tetragonal, and 71.3% cubic phases.[14] Some of the mechanical and thermal properties of this ceramic are summarized in Table I.[15] The disk specimens, 75 mm in diameter by 8 mm thick, were surface-finished by diamond-wheel grinding to an average roughness value of 0.2 ± 0.02 μm centerline average (CLA).

The counterface pins were made of

Table I: Mechanical and Thermal Properties of MgO-PSZ[15] and Ag.[18]*

Property	Unit	MgO-PSZ	Ag
Hardness	GPa	11	0.25
Fracture Toughness	MPa × $m^{1/2}$	7.6	–
Young's Modulus	GPa	205	71
Poisson's Ratio	–	0.31	0.37
Thermal Expansion (40-800°C) coefficient	10^{-6}/°C	10.3	19.1
Thermal Conductivity	W/m · K	3.08	420
Bulk density	kg/m^3	5,700	10,500
T-dependence of Modulus $(T_m/E)(dE/dT)$	–	0.5	0.5
T-dependence of Yield Strength $(T_m/\sigma_y)(d\sigma_y/dT)$	–	0.5	0.5
Melting Point	K	2893	1234
Thermal Capacity	J/kg · K	750	234
Latent Heat of Melting	kJ/kg	706	72
Yield Strength	MPa	–	54

*Definition of temperature-dependent material properties and typical values can be found in Reference 1.

https://doi.org/10.1557/S0883769400055834 Published online by Cambridge University Press

9.5 mm diameter balls with a surface finish of ≈0.03 μm CLA. All specimens were ultrasonically cleaned sequentially in hexane + 10 vol % toluene, acetone, deionized water containing 2 wt% laboratory detergent, and deionized water for about 1 min each, and then dried in an oven at 110°C for 20 min. This cleaning sequence was shown in Reference 16 to remove much of the organic contamination from the exposed surfaces of oxide ceramics.

Ion-Beam-Assisted Deposition of Silver

Thin silver films were formed by ion-beam-assisted deposition (IBAD) at room temperature in a vacuum chamber equipped with an electron-beam-heated evaporation source. Further details of this system and deposition procedures can be found in References 11–13. Prior to deposition of Ag, MgO-PSZ disks were sputter-cleaned by Ar ion bombardment. A 25 nm thick Ti layer was then produced on clean disk surfaces to help increase Ag film adhesion. Both the initial Ti layer and the Ag films were deposited under ion bombardment. The thickness of the resultant surface film was about 1.5 μm.

Friction and Wear Tests

Friction and wear tests were performed with pairs of MgO-PSZ/MgO-PSZ and MgO-PSZ/Ag-coated MgO-PSZ, at velocities ranging from 0.05 to 7.3 m/s. Two commercial pin-on-disk machines (Plint TE67 and CSEM-Tribometer) were used to cover the wide range of velocities. The specific test conditions are summarized in Table II. A 5 N load was used in all tests, creating an initial mean Hertzian contact pressure of ≈0.54 GPa for the MgO-PSZ test pairs. Frictional force was monitored by linear variable-displacement transducers and recorded on chart papers throughout the tests.

Wear-volume measurements on the balls used a mathematical expression suggested by Fischer and Tomizawa.[17] For better accuracy and reproducibility, two to four duplicate tests were run, and the average values with standard deviations are reported. Wear scars and tracks, as well as wear-debris particles, were examined by scanning electron microscopy.

Table II: Friction and Wear Test Conditions.

Parameters	Value
Load (N)	5.0
Sliding Velocity (m/s)	0.05 to 7.3
Relative Humidity (%)	45 ± 2
Sliding Distance (km)	2
Ambient Temperature (°C)	22 ± 1
Number of Tests	2 to 4
Tip Radius of Balls (mm)	4.75

Results and Discussion

Figure 1 shows the wear rates of MgO-PSZ balls sliding against uncoated and Ag-coated MgO-PSZ disks at different velocities. As is evident, wear increases sharply when the velocity is increased from 0.05 to 1 m/s. However, a slight decrease occurs when the velocity is further increased.

Microscopic examination of the sliding surfaces of MgO-PSZ balls revealed that at 1 m/s (where the highest wear rate was observed), wear was largely dominated by plastic flow, microcutting (see Figure 2a), and some microcracking (not shown in this micrograph). Wear-debris particles produced at this velocity were mostly flakelike fragments. Ball surfaces rubbed at velocities of 2 m/s and up contained features indicative of thermal cracking and local melting (see Figure 2b). Some plastic flow and/or smearing of asperity tips was also apparent on these surfaces. The molten MgO-PSZ seemed to have squeezed out of the sliding interfaces and accumulated around the trailing edges of the balls (see Figure 2c). Wear-debris particles found on and around the sliding surfaces consisted of large fragments and very fine debris particles (see Figure 2d). Large fragments appeared to have been produced by local melting of asperities and/or fine debris particles trapped at sliding interfaces.

As shown in Figure 1, Ag films substantially reduce the wear rates of MgO-PSZ balls at all sliding velocities tested in this study. For example, at 1 m/s, the average wear rate of balls sliding against the Ag-coated disks are reduced by a factor of ≈1,000 below that of balls slid against uncoated disks. The wear of Ag-coated disks was practically unmeasurable. Ag films remained intact on the rubbing surfaces following all the sliding tests. Wear appeared to have been confined to the asperity tips of underlying substrates.

As shown in Figure 3, the steady-state friction coefficients of test pairs without an Ag film are in the range of 0.65 to 0.75 at velocities up to 1 m/s. However, at much higher sliding velocities, friction coefficients decrease monotonically, reaching a value of ≈0.42 at 7.3 m/s. As for the pairs containing a Ag film, their friction coefficients are significantly lower and fluctuate between 0.30 and 0.35 at steady state.

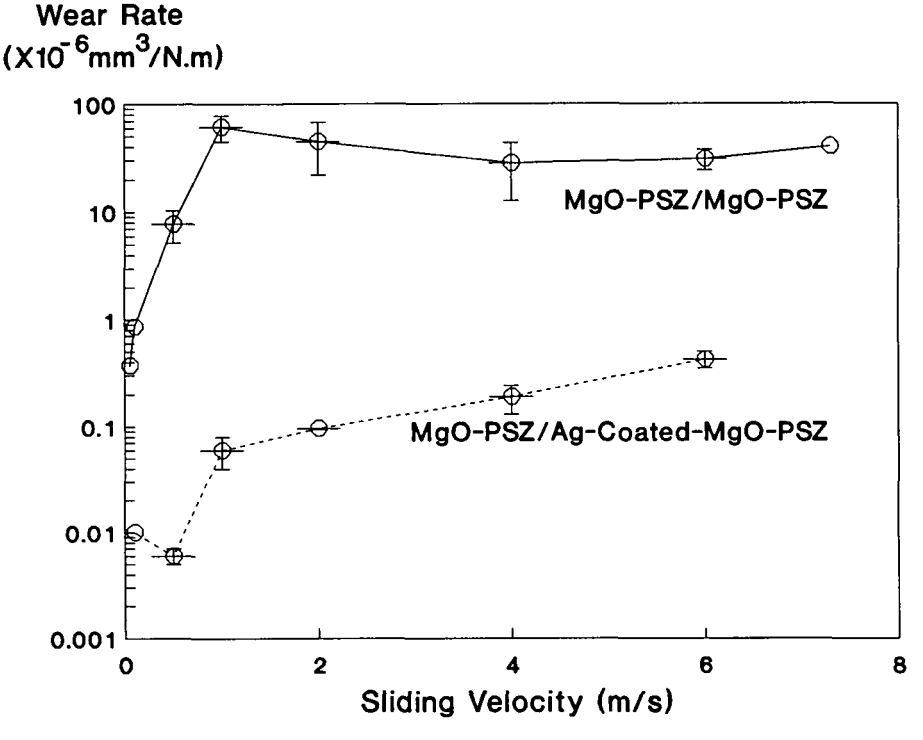

Figure 1. Variation of wear rate of MgO-PSZ balls sliding against uncoated and silver-coated MgO-PSZ disks, as a function of sliding velocity.

https://doi.org/10.1557/S0883769400055834 Published online by Cambridge University Press

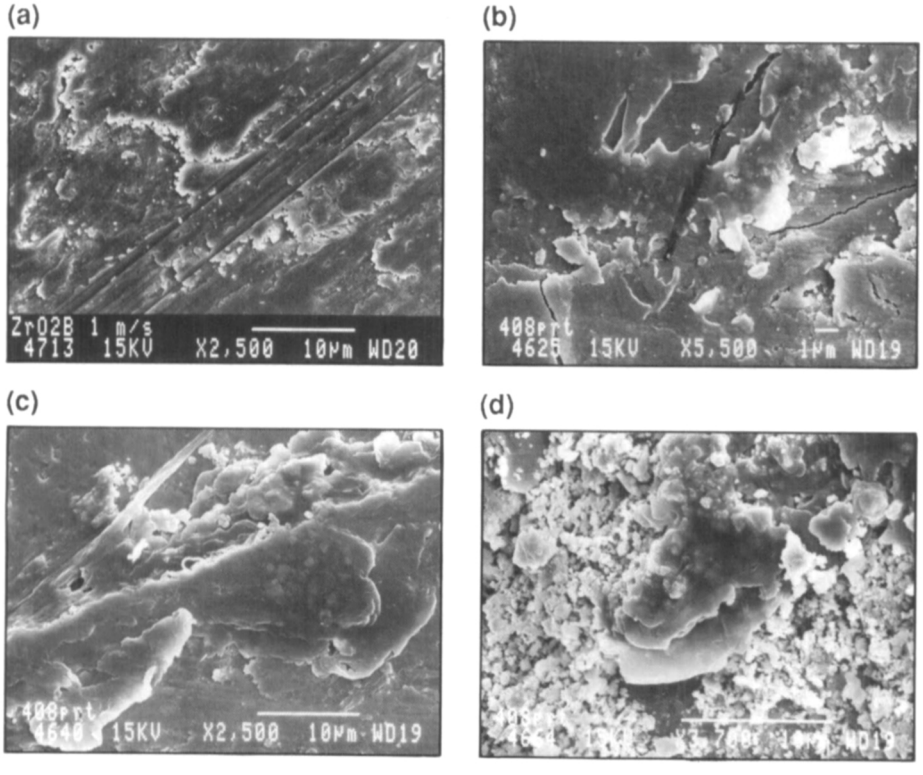

Figure 2. Scanning electron micrographs of wear scars of MgO-PSZ balls slid against the MgO-PSZ disk at (a) 1 m/s and (b-d) 6 m/s. Microfeatures shown in (a) are indicative of plastic flow and abrasive cutting but local melting is indicated in (b). Micrograph in (c) was taken from trailing edge of wear scar in (b) showing accumulation of molten material around edge. Micrograph in (d) shows flakelike wear fragments found around circular edges of wear scar in (b).

These results demonstrate that increasing velocity can have profound effects on the friction and wear behavior of MgO-PSZ ceramics. Furthermore, thin Ag films are very effective in reducing the wear of MgO-PSZ. The reduction in friction is also significant, especially at lower velocities. These observations are consistent with the original hypothesis that thin films of high thermal conductivity can indeed reduce the wear of insulating ceramics quite substantially.[12]

For the rapid increase in wear with increasing velocity, we propose the following explanation. As mentioned earlier, because of its very poor thermal conductivity (e.g., at 298 K, $k_{MgO\text{-}PSZ}$ = 3.08 W/m · K), MgO-PSZ cannot dissipate frictional heat rapidly from its sliding interfaces. As a result, hot spots may undergo thermal softening and can easily be smeared and/or deformed, as was seen in Figure 2a. Furthermore, steep temperature gradients that can develop between hot spots and surrounding regions can cause high thermal stresses to develop in and around the hot spots. When these thermal stresses are combined with normal and tangential stresses (due to applied load and frictional traction), microcracks can eventually develop and promote wear.

Using the *T-MAPS* software of Ashby et al.[1], we attempted to estimate the flash temperatures. Taking into account the materials properties given in Table I and test conditions in Table II, and for reasonable values of adjustable parameters, we constructed a series of temperature maps to show the magnitude of flash temperatures during sliding at velocities of 1, 2, and 4 m/s. The map in Figure 4 displays the variation of bulk (solid lines) and flash temperatures (dotted lines) over a wide range of pressure and sliding velocity. The data point is for our tests run at 2 m/s. For the test conditions and materials properties selected (see Table I), it is predicted that local asperity melting of MgO-PSZ becomes feasible at sliding velocities greater than ≈1.8 m/s, which is designated as the critical velocity v_c in Ashby's model. The map suggests that the magnitude of flash temperature would have been ≈1800°C at a velocity of 1 m/s, but at 4 and 6 m/s flash temperatures well in excess of the melting point of the MgO-PSZ used in this study are predicted.

Admittedly, such temperature estimates are notoriously variable and depend largely upon the particular choices of important parameters. It should be noted, however, that selected disposable parameters are similar to those deduced by Ashby et al.[1] from quantitative matching of theory and available experimental data for the ZrO_2 material. Thus, it is reasonable to say that our estimates have at least some semi-quantitative reliability.

In support of the predicted flash temperatures for MgO-PSZ/MgO-PSZ test pairs, scanning electron micrographs in Figure 2 reveal some evidence of plastic flow and microcutting on a surface rubbed at 1 m/s, but local melting on surfaces rubbed at much higher velocities. Deep groves and plastic flow seen in Figure 2a suggest that this surface was softened (possibly because of frictional heating), and thus could be scratched or deformed easily by harder particles and/or asperities. However, indications of local melting of those surfaces rubbed at much higher velocities suggest that at least the flash temperature of contact interfaces was on the order of the melting point of MgO-PSZ.

As is evident from Figure 2c, any molten portion of the MgO-PSZ is easily carried away and/or squeezed out of the sliding interface in the liquid and/or near-liquid state, after which it solidifies and accumulates around the trailing edges of the balls. Solidified portions can be broken or chipped away during sliding. The large fragments in Figure 2d are believed to have been formed by local melting, because they exhibit microfeatures indicative of melting.

The friction coefficients of MgO-PSZ/MgO-PSZ pairs decrease monotonically from ≈0.75 at 1 m/s to ≈0.42 at 7.3 m/s, and we believe this is due to local asperity melting at these high velocities. Recently, Ashby et al. proposed a semi-empirical model to describe the velocity-dependent frictional behavior of sliding pairs.[1] For velocities lower than that (v_0) at which the asperity temperature first exceeds the melting temperature (T_m), the friction coefficient (μ) is defined as

$$\mu = \mu_0$$

and for $v > v_0$

$$\mu = \mu_0 \exp - \{[\log(v/v_0)/\log(C_1)](1 - C_2 \log \tilde{F})\}$$

https://doi.org/10.1557/S0883769400055834 Published online by Cambridge University Press

where C_1 and C_2 are constants and were assigned values of 250 and 0.3 respectively, by Ashby et al.[1] based on experimental data for steel. $\bar{F}$ is the normalized pressure and is defined by Ashby et al.[1] as $\bar{F} = F/(H_0 A_n)$, where F is the normal load, H_0 is the hardness of MgO-PSZ at room temperature, and A_n is the nominal contact area.

Let us assume that the sliding velocity (v_0) at which local asperity melting began was 1.8 m/s and the corresponding μ_0 was 0.74. Using the empirical friction equation given above and the same values for C_1 and C_2, we find that at 2, 4, 6, and 7.3 m/s, the predicted friction coefficients are 0.71, 0.6, 0.45, and 0.39, respectively, whereas the real friction coefficient values for sliding MgO-PSZ couples were 0.72 at 2 m/s, 0.54 at 4 m/s, 0.46 at 6 m/s, and 0.42 at 7.3 m/s. It is clear that the predicted and measured friction values are quite comparable.

The present version of the *T-MAPS* software (i.e., Version 2.0) does not specifically handle coatings. However, to illustrate the rapid heat-dissipating effect of silver films, we attempted to estimate crudely the amount of flash heating for pairs containing a silver film. We assumed that thermal interactions at the sliding interfaces occur only between the uncoated MgO-PSZ pins and the Ag coating itself. This assumption may not hold for ultrathin films (e.g., those only a few nanometers thick) but may be considered reasonable for the thicknesses used in our case (i.e., 1.5 μm). Using the T-MAPS software, we generated a temperature map (Figure 5) for the sliding pair of MgO-PSZ/Ag-coated-MgO-PSZ. The flash temperatures predicted for pairs tested at 1, 2, 4, and 6 m/s, range from ≈30° to ≈100°C. When compared with the flash temperatures presented in the MgO-PSZ/MgO-PSZ temperature map (see Figure 4), the flash temperatures shown in Figure 5 are much lower, thus demonstrating that high-thermal-conductivity films can indeed have marked effects on the extent of frictional heating. Thermal and mechanical properties of Ag used to generate the temperature maps are given in Table I.[18] The data points indicate the tests conducted at 1, 2, 4, and 6 m/s.

It is again important to emphasize that this is a first attempt to account for the heat-dissipating effect of high-thermal-conductivity films. The results here should be used only to assess the expected flash temperatures because only short-range, lateral heat flow between asperity contact points is required to reduce asperity heating. For bulk-temperature estimates, the assumption of ZrO_2-ZrO_2 contact, as in Figure 4, is more appropriate because the bulk heating is determined by the long-range transport of heat through the ce-

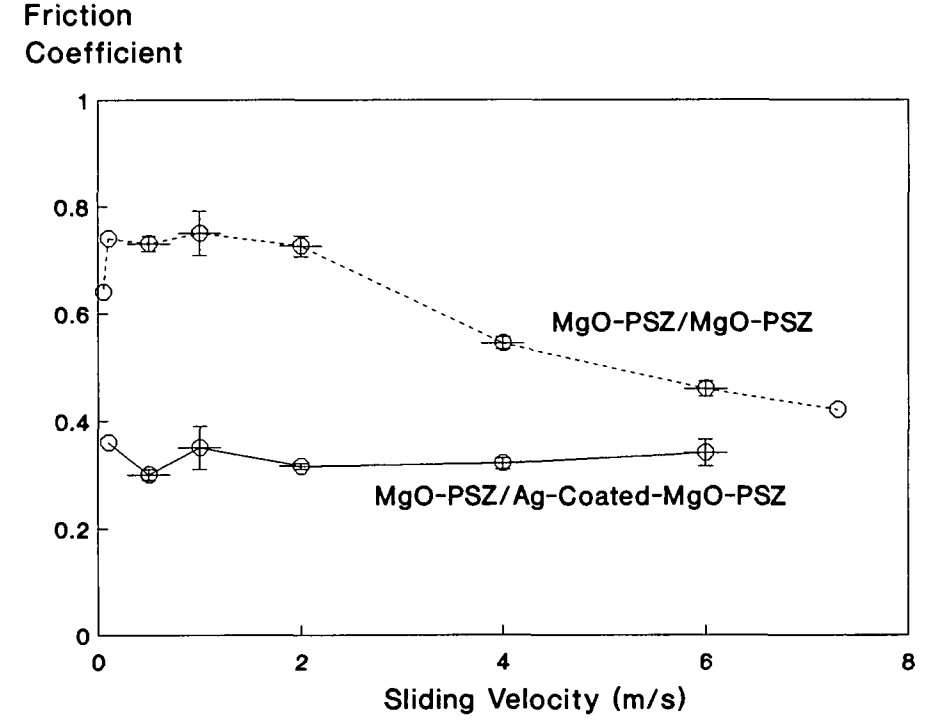

Figure 3. Friction coefficients of MgO-PSZ balls during sliding against uncoated and silver-coated MgO-PSZ disks at various velocities.

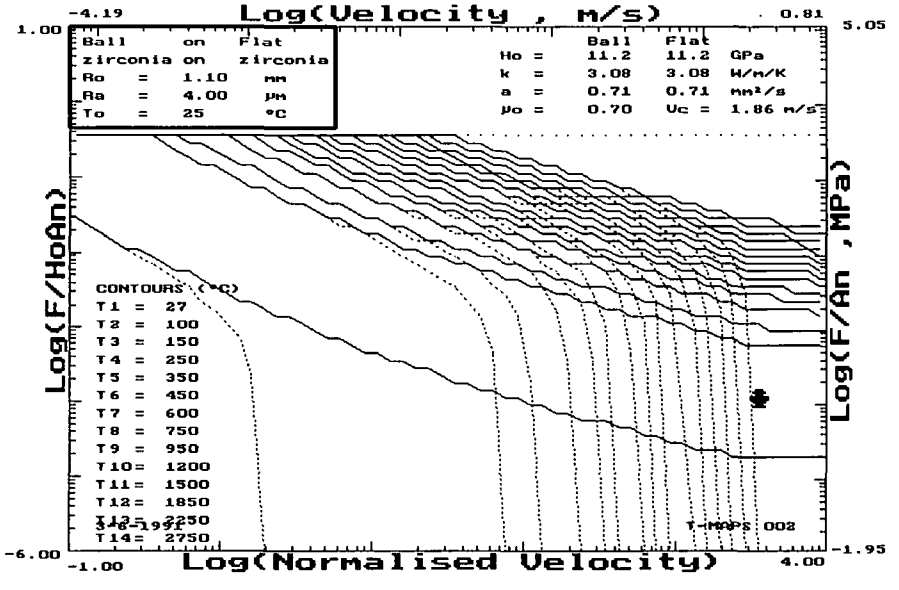

Figure 4. Temperature map of sliding pair of MgO-PSZ ball and disk. ♣ represents a test at 2 m/s. Solid lines represent bulk-temperature contours; broken lines represent flash-temperature contours. R_0 is nominal contact radius of circular wear scar; R_a, assigned radius of single isolated asperity junction; T_0, ambient temperature; H_0, hardness of MgO-PSZ at room temperature; k, thermal conductivity; a, thermal diffusivity; μ_0, friction coefficient; v_c, critical velocity (material properties are given in Table I).

https://doi.org/10.1557/S0883769400055834 Published online by Cambridge University Press

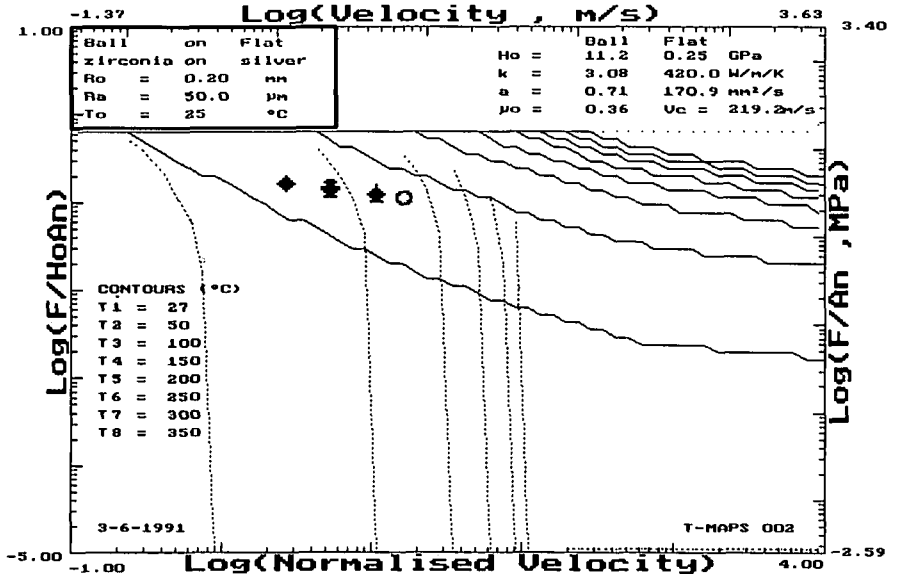

Figure 5. Temperature map of sliding pair of MgO-PSZ ball and silver-coated MgO-PSZ disk. ♦, ♣, ♠, and O represent experiments conducted at 1, 2, 4, and 6 m/s, respectively. R_0 is nominal contact radius (wear scar radius was approximately the same for cases used here); R_a, radius of single isolated asperity junction; T_0, ambient temperature; H_0, hardness at room temperature; k, thermal conductivity; a, thermal diffusivity; μ_0, friction coefficient; v_c, critical velocity.

ramic substrate to the heat sink where the specimen is secured to the test-machine frame.

Based on the temperature maps for uncoated and Ag-coated test pairs, and on the wear-test results, it is reasonable to conclude that the fast lateral dissipation of frictional heat from the local contact areas of ceramics is important for achieving lower wear rates. Therefore, the wear-controlling factor at high sliding velocities is closely related to the rapid lateral dissipation of frictional heat from asperity contacts.

Conclusions

Under the test conditions of this study, sliding velocity has significant effects on the friction and wear behavior of magnesia partially stabilized zirconia ceramics.

At lower velocities of up to 1 m/s, the friction coefficients were high and the wear rates of balls increased sharply with increasing velocity. However, at higher velocities, both friction and wear decreased first, but wear tended to increase again with further increasing velocity.

For the regime where friction fell monotonically, we found a good correlation between measured friction values and values predicted by an empirical friction model by Ashby et al.[1]

Electron microscopy inspection of the wear scars revealed some evidence of thermal cracking, plastic flow, and local melting, with the implication that these were the dominant mechanisms controlling the wear of MgO-PSZ ceramics.

We found that electron microscopy observations of worn surfaces correlated with the magnitude of flash temperatures estimated from the Ashby temperature maps.

Because of their very high thermal conductivity, silver films are very effective in reducing the wear of ceramics, especially at high sliding velocities. Also, they are effective in reducing the friction coefficient.

Acknowledgment

This work was supported by the Tribology Program, Office of Transportation Materials, U.S. Department of Energy, under Contract W-31-109-Eng-38.

References

1. M.F. Ashby, H.S. Kong, and J. Abulawi, *T-MAPS: A Program for Constructing Maps for Surface Heating in Unlubricated Sliding*, Version 2.0, (Cambridge University Engineering Department, Cambridge, U.K., 1990).
2. W.O. Winer and B-Y. Ting, *Development of a Theory of Wear of Ceramics*, Oak Ridge National Laboratory Report ORNL/84-7802/1 (1988).
3. B-Y. Ting and W.O. Winer, *ASME J. Tribol.* **111** (1989) p. 315.
4. T.F.J. Quinn, *ASLE Trans.* **21** (1978) p. 78.
5. A. Skopp, M. Woydt, and K-H. Habig, *Tribol. Int.* **23** (1990) p. 189.
6. K. Miyoshi, *Surf. Coat. Technol.* **36** (1988) p. 487.
7. A.F. Smith, *Wear* **96** (1984) p. 301.
8. M. Woydt and K-H. Habig, *Tribol. Int.* **22** (1989) p. 75.
9. I. Brikby, P. Harrison, and H. Stevens, *Ceram. Eng. Sci. Proc.* **9** (1988) p. 1431.
10. K.F. Dufrane and W.A. Glaeser, *Int. Conf. on Wear of Materials*, edited by K.C. Ludema (ASME, New York, 1987) p. 285.
11. A. Erdemir, D.E. Busch, R.A. Erck, G.R. Fenske, and R. Lee, *STLE Preprint No. 90-TC-1C-1.*
12. A. Erdemir, G.R. Fenske, R.A. Erck, and C.C. Cheng, *Lubr. Eng.* **46** (1990) p. 23.
13. A. Erdemir, G.R. Fenske, F.A. Nichols, and R.A. Erck, *Tribol. Trans.* **33** (1990) p. 511.
14. V. Aronov and M. Benetatos, *ASME Preprint No. 88-Trib-58, 1988.*
15. Materials Data Sheet, Nilcra Ceramics Pty., Ltd., Victoria, Australia.
16. R.S. Gates, J.P. Yellets, D.E. Deckman, and S.M. Hsu, *Selection and Use of Wear Tests for Ceramics*, edited by C.S. Yust and R.G. Bayer (ASTM, STP 1010, Philadelphia, 1988) p. 1.
17. T.E. Fischer and H. Tomizawa, *Wear* **105** (1985) p. 29.
18. *Metals Handbook*, 10th ed., **2** (ASM-International, Metals Park, OH, 1989) p. 699.

□

Materials Science and Education at the 1991 MRS Fall Meeting

Interested in helping enrich science education in your local schools? MRS wants to help you be effective and enjoy yourself in the process. Come to the Grassroots Education Networking Session at 7:30 p.m. on Tuesday, Dec. 3. And don't forget the one-day Workshop on Materials Education also being held on Tuesday, Dec. 3.

https://doi.org/10.1557/S0883769400055834 Published online by Cambridge University Press